catalysts

MDPI

Communication

The Green Synthesis of Biodiesel via Esterification in Water Catalyzed by the Phosphotungstic Acid–Functionalized Hydrophobic MCM–41 Catalyst

Dengke Li [1,2,3,4], Qinghao Shi [1,2,3], Fengbing Liang [1,2,3] and Dexin Feng [1,2,3,*]

[1] Key Laboratory of Biobased Materials, Qingdao Institute of Bioenergy and Bioprocess Technology, Chinese Academy of Sciences, Qingdao 266101, China; lidk@qibebt.ac.cn (D.L.); sqh_1st@163.com (Q.S.); liangfb@qibebt.ac.cn (F.L.)
[2] Shandong Energy Institute, Qingdao 266101, China
[3] Qingdao New Energy Shandong Laboratory, Qingdao 266101, China
[4] University of Chinese Academy of Sciences, Beijing 100049, China
* Correspondence: fengdx@qibebt.ac.cn

Abstract: Biodiesel is a non-toxic and environmentally friendly fuel that is made from renewable biological sources. It can replace petrochemical diesel and has very broad application prospects. However, the main raw materials in biodiesel are animal and plant oils, which present the problems of high costs and a lack of resources. The current research primarily emphasizes the transesterification process, with comparatively less focus on the esterification of fatty acids. In this paper, a series of phosphotungstic acid (PTA)-functionalized hydrophobic MCM–41 catalysts, OTS–PTA–MCM–41(C_x), were synthesized and used to catalyze the esterification of long-chain fatty acids with methanol in water. The experimental results show that the yield of esterification reached a maximum when catalyzed by OTS–PTA–MCM–41(C_x) and synthesized with a template agent with two carbon atoms less than the number of carbon atoms of a fatty acid. The effects of different reaction variables were investigated to optimize the reaction conditions for the maximum conversion. The stability of the catalyst was also verified. Finally, a mixed catalyst was used to catalyze in situ the esterification of fatty acids in a fermentation broth, which reached a high level (close to 90%). This paper provides references for the synthesis of a hydrophobic solid acid catalyst and green synthesis by esterification reactions in an aqueous solution and a fermentation broth system.

Keywords: biodiesel; solid acid; hydrophobic; heterogeneous catalysis; esterification reaction; water

Citation: Li, D.; Shi, Q.; Liang, F.; Feng, D. The Green Synthesis of Biodiesel via Esterification in Water Catalyzed by the Phosphotungstic Acid–Functionalized Hydrophobic MCM–41 Catalyst. *Catalysts* **2024**, *14*, 142. https://doi.org/10.3390/catal14020142

Academic Editor: Diego Luna

Received: 23 January 2024
Revised: 7 February 2024
Accepted: 8 February 2024
Published: 13 February 2024

1. Introduction

Recently, the heavy consumption of conventional fossil fuels and energy [1–3] has caused global warming and an energy crisis. Clean and renewable biodiesel has been greatly developed and promoted to deal with global warming and energy shortages [4]. It is widely considered an important renewable energy source and one of the keys to the development of new energy [5,6]. Biodiesel is usually obtained through the transesterification of vegetable oil with short-chain alcohols [7–9]. The existing synthesis methods have many disadvantages, such as the use of expensive and scarce raw materials. In contrast, fatty acids synthesized by microbial fermentation have great potential to produce biodiesel as a raw material [10,11]. The advantages of microbial fermentation in synthesizing fatty acids include renewability, a short production cycle, and environmental friendliness. However, due to the inhibition of H_2O during the esterification and mass transfer processes [12–15], the extraction and separation of fatty acids from the fermentation broth are necessary, which are complex and expensive. In addition, the use of organic solvents violates the concept of green chemistry and increases the cost of products, which is not conducive to their later industrial applications. Researchers have explored the synthesis of biodiesel

through biological pathways, but the yield and efficiency remain at a low level [16,17], so it cannot replace chemical methods at the current stage [18]. In the chemical synthesis method, organic solvent systems play a central role [19,20]. Research on the synthesis of fatty acid esters in an aqueous solution is very scarce. The study of new hydrophobic catalysts is crucial for achieving esterification in green aqueous solvents. Currently, heterogeneous catalysts with Bronsted acidity, such as heteropolyacid, molecular sieves, and cation exchange resin, have attracted wide attention for the preparation of fatty acid esters by catalyzing reactions of fatty acids and alcohols [21–24]. For example, Zhang et al. [23] reported a heteropolyacid/Ni–MOF composite catalyst to catalyze the formation of fatty acid methyl ester between fatty acids and methanol through an esterification reaction, and the synthesized catalyst exhibited good catalytic performance. The maximum conversion rate for oleic acid reached 86.1% in methanol. Guo et al. [24] designed and synthesized a heterogeneous $H_6PV_3MoW_8O_{40}$/AC–Ag catalyst to catalyze the synthesis of biodiesel. The yield of biodiesel is 92% when using methanol as the solvent. The above heterogeneous catalyst realized an esterification reaction in organic solvents, and the heteropolyacid catalyst showed excellent catalytic performance. However, the high solubility of heteropolyacid in water is also an urgent problem that needs to be solved [25]. The application of heteropolyacid to esterification in aqueous solutions while maintaining good catalytic performance is the focus of current research, and it is also the key to achieving the high-value derivatization of fatty acids in water. In order to solve the existing problems and research focus mentioned above, a series of hydrophobic and PTA-functionalized MCM–41 catalysts (OTS–PTA–MCM–41(C_x)) were designed, synthesized, and characterized in detail. Heteropolyacid can effectively catalyze esterification reactions, and the hydrophobic alkyl group can promote the mass transfer process of fatty acids in a catalyst and inhibit the leaching of heteropolyacid in water by reducing the adsorption of H_2O in that catalyst [26,27]. The synthesized catalysts (OTS–PTA–MCM–41(C_x)) exhibited excellent performance in catalyzing the esterification of long-chain fatty acids with methanol in water and a fermentation broth, which can be applied to the in situ synthesis of biodiesel through an esterification reaction in a fermentation broth system. A summary of previous studies and the contents of this paper are shown in Scheme 1.

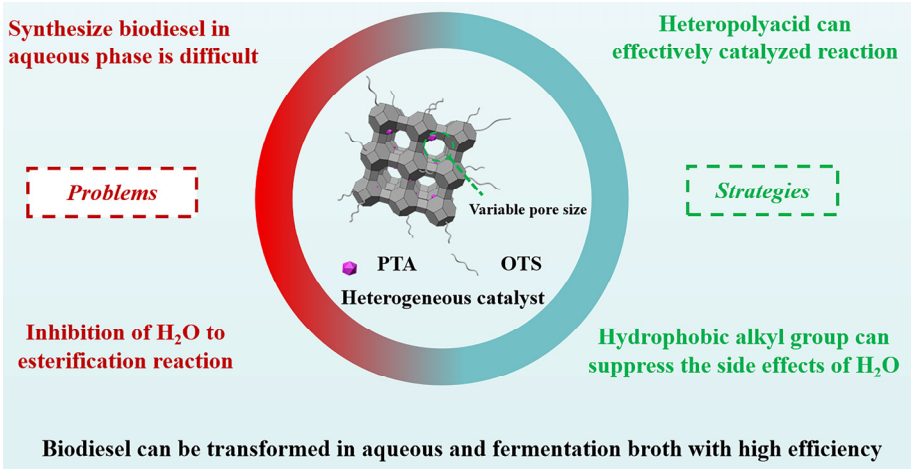

Scheme 1. The current problems in the aqueous synthesis of biodiesel and the corresponding strategies in this paper.

2. Results

Here, we aimed to synthesize the target catalyst by loading the heteropolyacid in the molecular sieve, MCM–41, with a different template agent. During the synthesis process, micelles appeared in the synthesis system after adding the surfactant and adjusting the pH. The hydrophobic end of the surfactants aggregated in the aqueous medium, exposing hydrophilic ends, and the SiO_4^{4-} ions formed by TEOS showed a negative charge

outside the micelles. The negatively charged heteropolyacid component accumulated in the interlayer between the hydrophilic end of the surfactants and SiO_4^{4-} under the synergistic effect of electrostatic force and surface tension. In the subsequent calcination process, the heteropolyacid interacted with the freshly synthesized MCM–41 to form the catalyst with a stable structure [28]. Figure 1 shows the XRD patterns of PTA–MCM–41(C_x). A wide peak can be found at 23°, which is attributed to the amorphous silica in the pore of the MCM–41 [29]. The sharp diffraction peaks at 30.61° and 26.36° represent the PTA dispersed in MCM–41 [30,31]. These results confirm that PTA molecules are dispersed in the pores and surfaces of MCM–41 zeolite. The diffraction peak at 27° decreases with the increase in the carbon chain of the template agent C_xTAB. With a shorter chain template agent, the synthesized molecular sieve exhibits a larger specific surface area, leading to the more dispersed distribution of heteropolyacids [32].

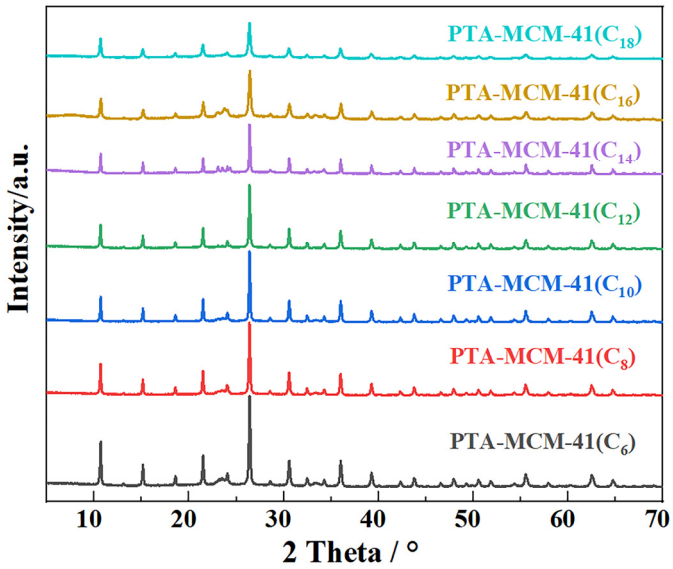

Figure 1. XRD patterns of PTA–MCM–41(C_x).

The successful loading of PTA on the MCM–41 molecular sieve can also be confirmed by FT–IR, as shown in Figure 2a. Strong diffraction peaks are observed at 1081 cm^{-1} for the vibration of Si–O–Si in all PTA–MCM–41(C_x) catalysts [33], and the characteristic peak of heteropolyacid was at 1065 cm^{-1}, which was caused by the asymmetric vibration of PTA with absence [34]. The characteristic peaks at 989, 876, and 800 cm^{-1} are attributed to W–O, W–O_b–W, W–O_c–W bonds, respectively. These characteristic peaks are the characteristics of a Keggin-type phosphotungstic acid structure [35,36]. Figure 2b displays the FT–IR spectra of the PTA–MCM–41(C_{14}) before and after the hydrophobic modification. It can be observed that there were diffraction peaks at 2855 cm^{-1} and 2925 cm^{-1} in the OTS–PTA–MCM–41(C_{14}) catalyst after hydrophobic modification, which can be attributed to the C–H bond of symmetric methylene and antisymmetric methylene in OTS attached to the MCM–41 [37]. During the hydrophobic functionalized process, the trichlorooctadecylsilane with a large steric hindrance group interacts with the hydroxyl group of MCM–41 to attach the hydrophobic group on the external surface of MCM–41 [37,38]. The results of XRD and FT–IR show that the designed catalyst, OTS–PTA–MCM–41(C_x), was successfully synthesized. With heteropolyacid and hydrophobic alkyl groups, the catalysts are expected to exhibit excellent catalytic performance.

Figure 3 shows the N_2 physical adsorption–desorption isotherm of OTS–PTA–MCM–41(C_{14}). With the feature of reversibility at P/P_0 in the range of 0.20 to 0.45, the isotherm of OTS–PTA–MCM–41(C_{14}) is an IV isotherm [39,40]. The specific surface area of OTS–PTA–MCM–41(C_{14}) is 6.44 cm^2/g, which exhibit a significant decrease compared with MCM–41(C_{14}) (11.86 m^2/g). This result indicates the weak interaction between adsorbents and

absorbers, which can be interpreted as phosphotungstic acid being filled in the channels of the molecular sieve, resulting in blocking and the reduction in the specific surface area. This result is consistent with the XRD and FT–IR assessments, indicating that the heteropolyacid is successfully introduced into the molecular sieve MCM-41.

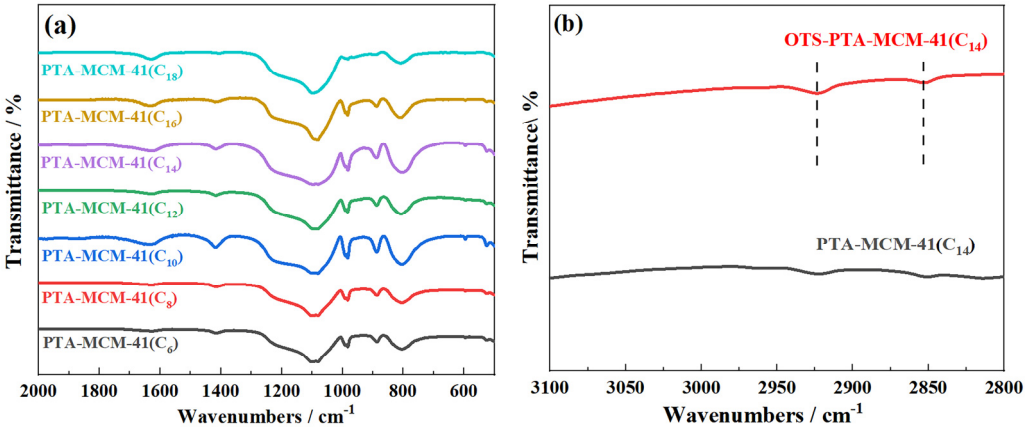

Figure 2. FT–IR spectrums of (**a**) PTA–MCM–41(C_x), (**b**) PTA–MCM–41(C_{14}), and OTS–PTA–MCM–41(C_{14}).

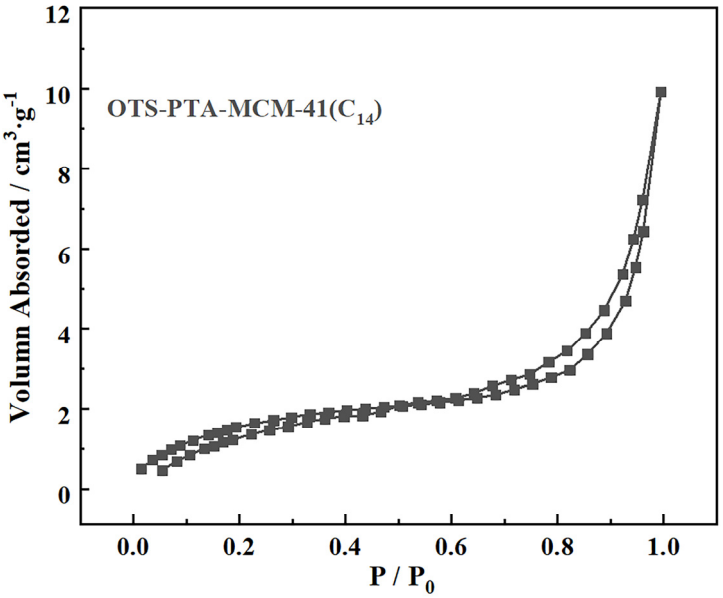

Figure 3. N_2 physisorption isotherms of OTS–PTA–MCM–41(C_{14}).

Figure 4 displays the TEM and SEM spectra of OTS–PTA–MCM–41(C_{14}). It is a round cluster structure similar to a sphere with good dispersion and crystallinity. Each spherical cluster is about 200–400 nanometers in diameter. There are uniformly distributed channels on the surface of the molecular sieve, and the diameter is about a few nanometers. Due to the small size, the PTA and the C_xTAB cannot be observed.

Thermal stability is an important criterion used to evaluate the catalysts. TG curves of PTA–MCM–41(C_{14}) and OTS–PTA–MCM–41(C_{14}) are shown in Figure 5. A slight weight reduction in the catalyst before 200 °C is caused by the evaporation of free water adsorbed in the catalyst [41]. The decline in the range of 200–600 °C can be attributed to the partial dissociation of OTS and PTA [42,43], which indicates the phosphotungstic acid and OTS formed a strong connection with MCM–41 in the catalyst. Experimental results show that the designed catalyst has good stability under a reaction temperature and can efficiently and continuously catalyze the reaction.

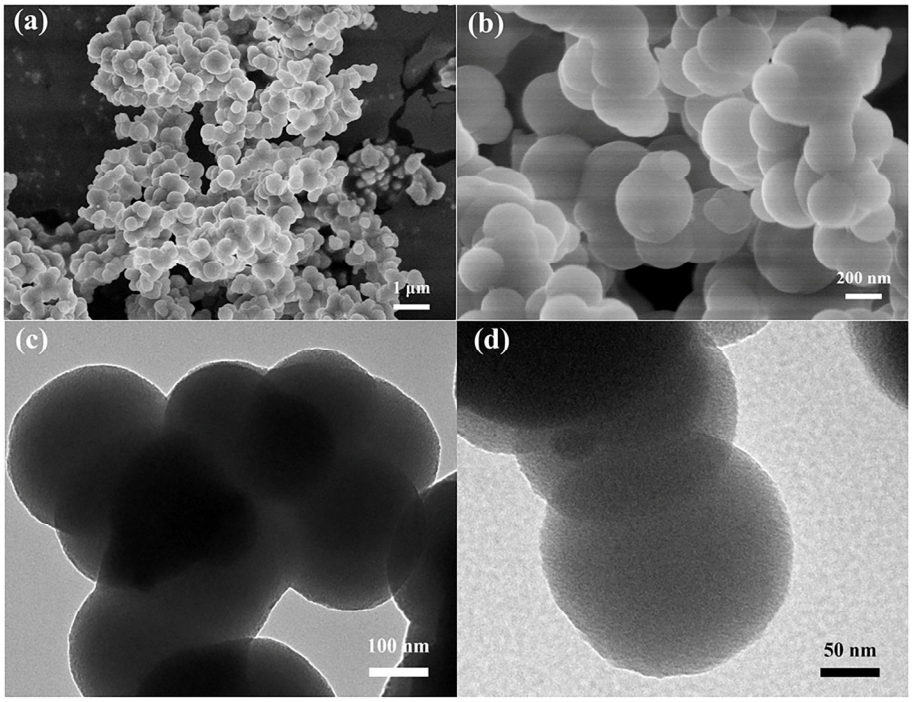

Figure 4. (**a**,**b**) SEM and (**c**,**d**) TEM images of OTS–PTA–MCM–41(C_{14}).

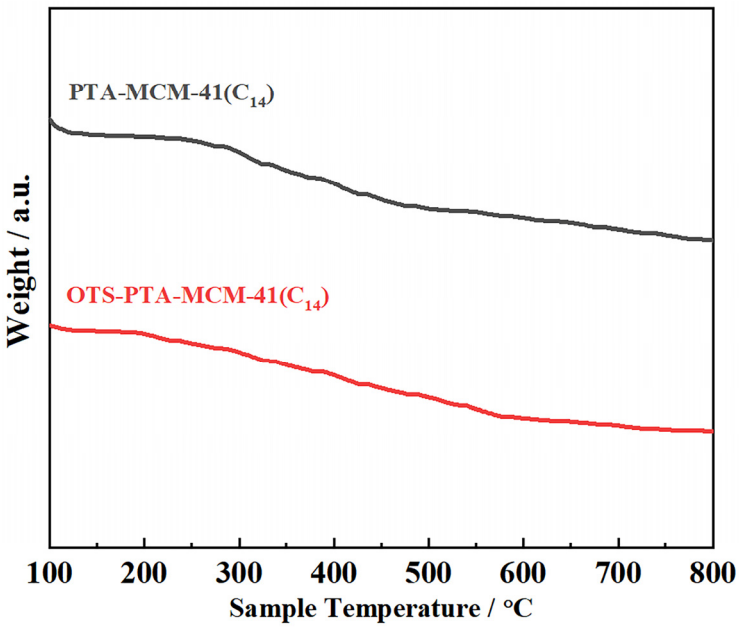

Figure 5. TG curves of PTA–MCM–41(C_{14}) and OTS–PTA–MCM–41(C_{14}).

The acidity of catalysts was tested by NH_3–TPD. The amount of acid sites of MCM–41(C_{14}), PTA–MCM–41(C_{14}), and OTS–PTA–MCM–41(C_{14}) are 0.61, 1.03, and 1.01 mmol/g, respectively. The results show that the support of PTA greatly increases the number of acidity sites in MCM–41. It can be observed from the NH_3–TPD curve in Figure 6 that there is an obvious desorption peak below 180 °C in MCM–41(C_{14}) and OTS–PTA–MCM–41(C_{14}), which represents the weak acidic hydroxyl group in MCM–41. Notably, an obvious signal appears in the high-temperature range of 500–540 °C, which corresponds to phosphotungstic acid with strong Bronsted acidity introduced into MCM–41. This curve is consistent with FT–IR and XRD results, indicating that the catalyst with strong Bronsted acidity heteropolyacid can effectively promote the reaction. Although the introduction of

OTS slightly hides the acid sites, the hydrophobicity of the catalyst is obviously improved. This modification can effectively promote the transfer of reactants in the catalyst, inhibit the adverse effects of H_2O during the reaction, and improve the reaction effect.

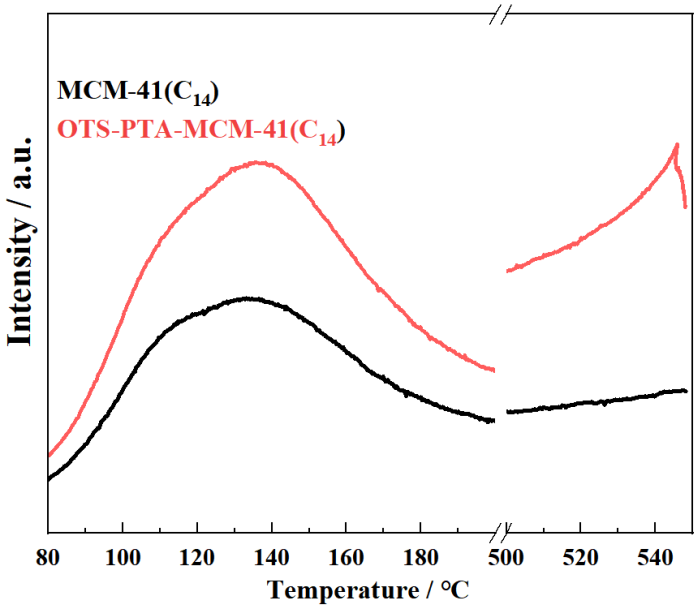

Figure 6. NH_3–TPD curves of MCM–41(C_{14}) and OTS–PTA–MCM–41(C_{14}).

The methyl esterification reaction of long-chain fatty acids (number of carbon atoms = 12, 14, 16) was used to test the catalytic performance of synthesized catalysts; the results are displayed in Table 1. The esterification yields of the three fatty acids basically increase with the increase in carbon chains of the C_xTAB template agent whether the catalyst is hydrophobic or not. Interestingly, for each fatty acid, there is a corresponding catalyst with the best catalytic activity. This can be summed up as the n–2 rule, which means that the catalyst, PTA–MCM–41(C_x), synthesized by C_xTAB with n–2 carbons on the long alkyl chain, displays the best catalytic performance in the esterification of fatty acid containing n carbon atoms. For example, methyl palmitate of yield reaches the highest value catalyzed by PTA–MCM–41(C_{14}). The reason for this rule may be the selective entry of fatty acids into catalysts with different pore sizes. The pore size of catalysts synthesized by n–2 C_xTAB is suitable for the diameter of the corresponding fatty acid with n carbon, leading to the increase in selectivity and yield. At the same time, we observe that the introduction of the OTS hydrophobic group can improve the catalytic performance of the catalyst, but the effect is limited. The reason is that the active center in the catalyst is phosphotungstic acid; hydrophobic groups do not directly participate in the reaction process as active centers but improve the reaction conditions. The introduction of hydrophobic groups will weaken the absorption of H_2O on the external surface of the catalyst, which can promote the transfer of the reactants and product and improve the reaction effect.

Based on previous experiments, OTS–PTA–MCM–41(C_{14}) displayed good catalytic activity in the methyl esterification of palmitic acid (C_{16}). Subsequently, some experiments were conducted to optimize reaction conditions. Reaction conditions consist of catalyst dosage, reaction temperature, and time. The experimental results are shown in Table 2. A blank test is first conducted to verify the key role of the catalyst in the reaction. Next, the amount of catalyst in the reaction was investigated. It can be seen from entries 2–6 that the highest yield of methyl palmitate was achieved when adding 150 mg of catalyst. In entries 7–11, the temperature range is 70–150 °C; the yield of methyl palmitate firstly increases and then decreases with the increase in temperature. This can be attributed to the fact that esterification is endothermic [44,45] and reversible, and the increase in temperature shifts the equilibrium toward the positive reaction, resulting in an increase in yield. In entries

11–14, the temperature exceeded 150 °C, and the yield of methyl palmitate slowly decreased with the increase in temperature. The reason for this is that the reaction is restrained at an excessive temperature. Entries 15–20 show the effect of time; it can be observed that the yield of palmitic acid is the highest at 3 h. When the reacion time is prolonged, the synthesized methyl palmitate starts decomposition, resulting in a decrease in product yield.

Table 1. Preparation of biodiesel in different conditions catalyzed by various catalysts in water.

Entry	Catalyst	Solvent	Conditions [1]			Yield (%)		
			T (°C)	t (h)	C [2] (mg)	L [3]	M [4]	P [5]
1	PTA–MCM–41(C_6)	water	70	3	100	63.2	64.8	60.1
2	PTA–MCM–41(C_8)	water	70	3	100	64.8	62.7	64.2
3	PTA–MCM–41(C_{10})	water	70	3	100	67.1	66.9	67.4
4	PTA–MCM–41(C_{12})	water	70	3	100	66.9	74.3	68.7
5	PTA–MCM–41(C_{14})	water	70	3	100	67.0	74.4	71.8
6	PTA–MCM–41(C_{16})	water	70	3	100	65.2	72.8	70.4
7	PTA–MCM–41(C_{18})	water	70	3	100	65.2	73.0	71.1
8	OTS–PTA–MCM–41(C_6)	water	70	3	100	65.4	67.7	63.2
9	OTS–PTA–MCM–41(C_8)	water	70	3	100	68.2	68.3	67.8
10	OTS–PTA–MCM–41(C_{10})	water	70	3	100	72.1	69.9	67.7
11	OTS–PTA–MCM–41(C_{12})	water	70	3	100	71.2	76.5	70.2
12	OTS–PTA–MCM–41(C_{14})	water	70	3	100	72.6	76.6	74.4
13	OTS–PTA–MCM–41(C_{16})	water	70	3	100	71.1	74.3	71.1
14	OTS–PTA–MCM–41(C_{18})	water	70	3	100	71.2	74.8	72.3

[1] Conditions: 100 mg of various acids, 5 mL of methanol, 45 mL of water, and 500 rpm stirring rate. [2] C: Catalyst dosage. [3] L: Methyl lauric. [4] M: Methyl myristic. [5] P: Methyl palmitate.

Table 2. Esterification in different conditions catalyzed by OTS–PTA–MCM–41(C_{14}) in water.

Entry	Catalyst	Solvent	Conditions [1]			Yield (%)
			T (°C)	t (h)	C [2] (mg)	Methyl Palmitate
1	OTS–PTA–MCM–41(C_{14})	water	150	3	/	35.6
2	OTS–PTA–MCM–41(C_{14})	water	150	3	50	78.2
3	OTS–PTA–MCM–41(C_{14})	water	150	3	100	88.0
4	OTS–PTA–MCM–41(C_{14})	water	150	3	150	93.0
5	OTS–PTA–MCM–41(C_{14})	water	150	3	200	92.7
6	OTS–PTA–MCM–41(C_{14})	water	150	3	250	91.9
7	OTS–PTA–MCM–41(C_{14})	water	70	3	150	74.4
8	OTS–PTA–MCM–41(C_{14})	water	90	3	150	75.9
9	OTS–PTA–MCM–41(C_{14})	water	110	3	150	86.1
10	OTS–PTA–MCM–41(C_{14})	water	130	3	150	89.8
11	OTS–PTA–MCM–41(C_{14})	water	150	3	150	93.0
12	OTS–PTA–MCM–41(C_{14})	water	170	3	150	91.2
13	OTS–PTA–MCM–41(C_{14})	water	190	3	150	90.5
14	OTS–PTA–MCM–41(C_{14})	water	210	3	150	91.1
15	OTS–PTA–MCM–41(C_{14})	water	150	1	150	55.7
16	OTS–PTA–MCM–41(C_{14})	water	150	3	150	93.0
17	OTS–PTA–MCM–41(C_{14})	water	150	6	150	82.0
18	OTS–PTA–MCM–41(C_{14})	water	150	9	150	82.5
19	OTS–PTA–MCM–41(C_{14})	water	150	12	150	90.9
20	OTS–PTA–MCM–41(C_{14})	water	150	24	150	84.2

[1] Conditions: 100 mg of various acids, 5 mL of methanol, 45 mL of water, and 500 rpm stirring rate. [2] C: Catalyst dosage.

After the optimization of reaction conditions, the yield of methyl palmitate catalyzed by the OTS–PTA–MCM–41(C_{14}) catalyst reached as high as 93.0%. Combined with the previous n–2 rule, the optimal reaction conditions of OTS–PTA–MCM–41(C_{10}) and OTS–

PTA–MCM–41(C_{12}) to catalyze lauric acid, myristic acid can also be inferred. The reaction conditions are as follows: 150 mg catalyst is added to the reaction system for 3 h under 150 °C.

The stability of catalysts is also important for their industrial applications [46]. For this purpose, the cycling performance test of OTS–PTA–MCM–41(C14) was carried out. The experimental conditions are the same as before; the performance of the catalyst after cycling five times is shown in Figure 7. The yield of methyl palmitate decreases from 93.0% to 90.9%, which can be caused by the partial dissociation of PTA and OTS in the catalyst. Results prove that OTS–PTA–MCM–41(C_{14}) exhibits excellent stability. The introduction of the hydrophobic OTS group improves the hydrophobicity of the catalyst by reducing the adsorption of H_2O in the catalyst and effectively prevents the leaching of the heteropolyacid, thus maintaining a stable and efficient catalytic performance.

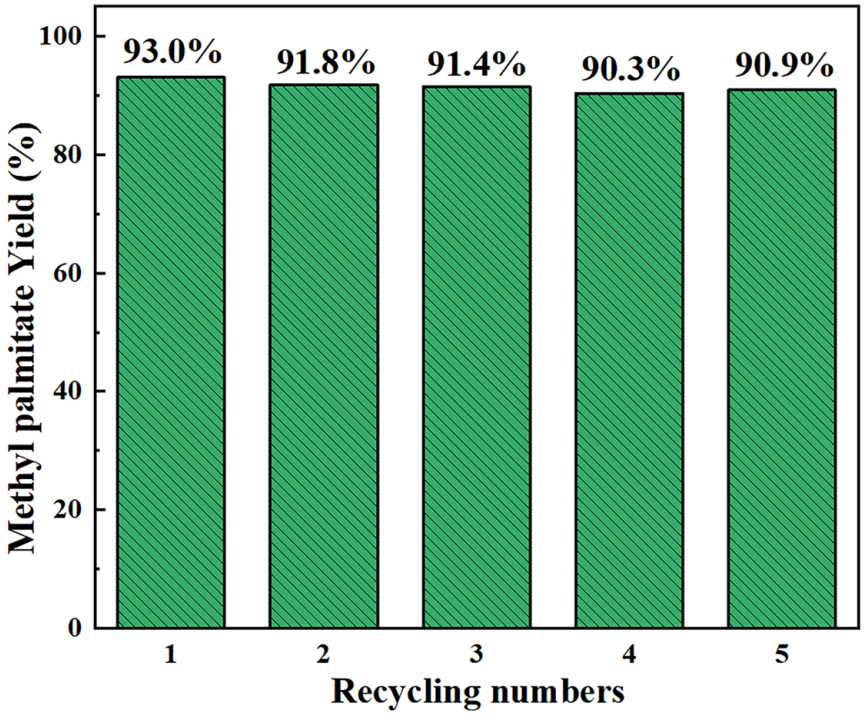

Figure 7. Cycling performance of OTS–PTA–MCM–41(C_{14}).

Next, the synthesized catalyst was used to catalyze the in situ esterification in fermentation broth. Firstly, GC detection of the existing fermentation broth system was carried out. The concentration of lauric acid, myristic acid, and palmitic acid in the fermentation broth was 18.98 mg/L, 51.95 mg/L, and 13.66 mg/L, respectively.

In the fermentation broth mentioned before, synthesized catalysts were used to catalyze the esterification of three fatty acids, and the results are shown in Table 3. It can be observed that the n–2 rule still holds. The esterification yield of the three kinds of acids in the fermentation broth catalyzed by the same catalyst was higher than the corresponding yield in water. A possible reason for this result is the addition of sodium dodecyl benzene sulfonate in the fermentation broth. The phase-transfer reagent can promote cell wall fragmentation and improve the transfer process of the esterification reaction. Firstly, the addition of surfactant changes the interfacial properties of water and has the emulsified effect in fermentation broth. Secondly, the addition of surfactant increases the solubilization of three fatty acids in fermentation broth. In addition, it also facilitates the dispersion of the reaction system, making fatty acids disperse more uniformly and become easier to contact with the catalyst.

According to the conclusions obtained, experiments were conducted to test the catalytic activity of the catalyst in the esterification of three fatty acids in the fermentation

broth, as shown in Table 4. The reactions in entries 1–3 are catalyzed by a single catalyst, which confirms the n–2 rule. In the entry 4 reaction, the mixed catalyst was used to catalyze the methyl esterification of the three acids. For each fatty acid, the catalyst with the best catalytic performance was selected according to the n–2 rule. The amount of three catalysts was utilized according to the concentration of three fatty acids in the fermentation broth. The concentration of lauric acid, myristic acid, and palmitic acid is 18.98 mg/L, 51.95 mg/L, and 13.66 mg/L. The corresponding amount of OTS–PTA–MCM–41(C_{10}), OTS–PTA–MCM–41(C_{12}), and OTS–PTA–MCM–41(C_{14}) is 33.75 mg, 90.75 mg, and 25.5 mg, respectively. At optimal reaction conditions, the yields of methyl laurate, methyl myristate, and methyl palmitate reached 91.9%, 89.7%, and 91.2%, which achieved efficient in situ esterification in the fermentation broth. However, the yield of fatty acids in fermentation broth catalyzed by mixed catalyst did not achieve the expected maximum value. This might be caused by the pore size of mixed catalysts. For example, the pore size of OTS–PTA–MCM–41(C_{10}) is relatively small, and palmitic acid does not easily enter into the pore, resulting in the yield of methyl palmitate being lower than that catalyzed by a single OTS–PTA–MCM–41(C_{14}). In general, the product yields reached a high level.

Table 3. Preparation of biodiesel catalyzed by PTA–MCM–41(C_x) in fermentation broth.

Entry	Catalyst	Solvent	Conditions [1]			Yield (%)		
			T (°C)	T (h)	C [2] (mg)	L [3]	M [4]	P [5]
1	PTA–MCM–41(C_6)	water	70	3	100	71.4	74.1	59.1
2	PTA–MCM–41(C_8)	water	70	3	100	76.4	73.2	70.3
3	PTA–MCM–41(C_{10})	water	70	3	100	85.9	79.8	73.6
4	PTA–MCM–41(C_{12})	water	70	3	100	84.7	84.8	80.5
5	PTA–MCM–41(C_{14})	water	70	3	100	83.8	84.1	86.4
6	PTA–MCM–41(C_{16})	water	70	3	100	83.5	84.3	81.9
7	PTA–MCM–41(C_{18})	water	70	3	100	83.0	83.7	82.3

[1] Conditions: 100 mg of various acids, 5 mL of methanol, 45 mL of water, and 500 rpm stirring rate. [2] C: Catalyst dosage. [3] L: Methyl lauric. [4] M: Methyl myristic. [5] P: Methyl palmitate.

Table 4. Esterification of fermentation broth catalyzed by OTS–PTA–MCM–41(C_x).

Entry	Catalyst and Dosage			Solvent	Conditions [1]		Yield (%)		
	C_a [2]	C_b [3]	C_c [4]		T (°C)	t (h)	L [5]	M [6]	P [7]
1	150	/	/	water	150	3	92.9	83.8	86.4
2	/	150	/	water	150	3	90.6	92.1	89.4
3	/	/	150	water	150	3	91.7	86.6	92.1
4	33.75	90.75	25.5	water	150	3	91.9	89.7	91.2

[1] Conditions: 100 mg of various acids, 5 mL of methanol, 45 mL of water, and 500 rpm stirring rate. [2] C_a: OTS–PTA–MCM–41(C_{10}), [3] C_b: OTS–PTA–MCM–41(C_{12}), [4] C_c: OTS–PTA–MCM–41(C_{14}). [5] L: Methyl lauric. [6] M: Methyl myristic. [7] P: Methyl palmitate.

Finally, the general reaction process catalyzed by the OTS–PTA–MCM–41(C_x) is illustrated in Scheme 2. Heteropolyacid can effectively catalyze the esterification reaction; the hydrophobic alkyl group OTS located on the surface of the molecular sieve can promote the transfer of fatty acid in the catalyst and inhibit the leaching of heteropolyacid [37,45]. Consequently, fatty acids and methanol can more easily enter the inside of the catalyst to proceed with the esterification reaction catalyzed by heteropolyacid in OTS–PTA–MCM–41(C_x).

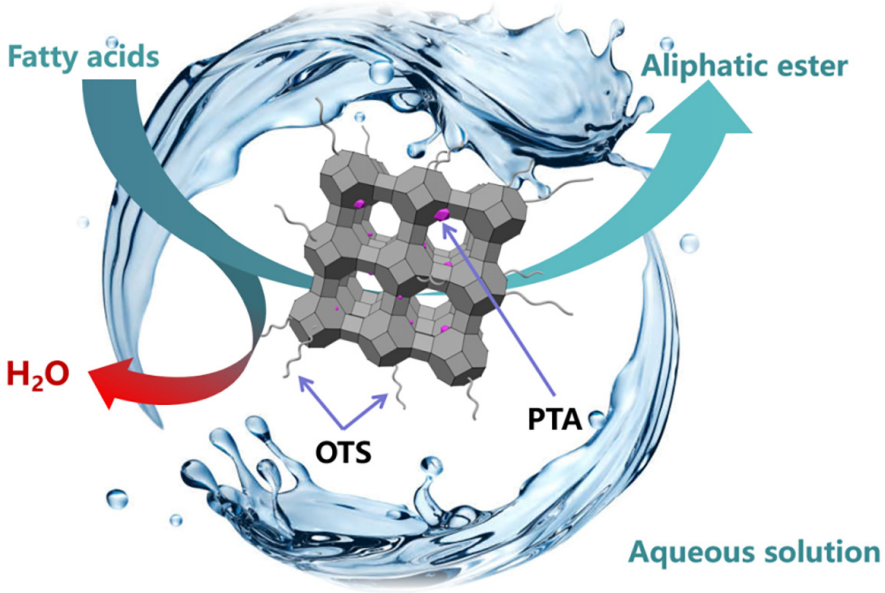

Scheme 2. The esterification of fatty acid catalyzed by OTS–PTA–MCM–41(C_x) in water.

3. Materials and Methods

3.1. Synthesis of Catalysts

Methanol, sodium phosphate tribasic dodecahydrate, sodium tungstate dihydrate, tetraethyl orthosilicate, ammonia solution, hydrochloric acid, acetonitrile, toluene, trichlorooctadecylsilane, and ethanol were purchased from Sinopharm Chemical Reagent Co., Ltd. (Shanghai, China). Alkyl trimethyl ammonium bromide (number of carbons on alkyl chain = 6, 8, 10, 12, 14, 16, and 18), methyl laurate, methyl myristate, methyl palmitate, and methyl arachidate were purchased from Aladdin Reagent Co., Ltd. (Shanghai, China). All purchased materials did not require further separation and purification.

The synthesis procedure of $(C_xTA)_4H_3[PW_{11}(H_2O)O_{39}]\cdot nH_2O$ was as follows. 3 mmol Na_2HPO_4 and 30 mmol $Na_2WO_4\cdot 2H_2O$ were dissolved in 200 mL water. Then, 20 mL C_xTAB (x is the number of C atoms, 45 mmol) of aqueous solution was dropped in at 80–85 °C under stirring. The formed solid was filtered out and recrystallized in a mixture of water and acetonitrile(V_{Water}:V_{MeCN} = 1:1) to obtain $(C_xTA)_4H_3[PW_{11}(H_2O)O_{39}]\cdot nH_2O$. (x represents the number of carbon atoms on the alkyl group in template agent, x = 6, 8, 10, 12, 14, 16, and 18).

PTA–MCM–41(C_x) was synthesized by the following procedures from [28] with some modifications. C_xTAB (5.95 mmol) was dissolved in a mixture of deionized water (20 mL), ethanol (62 mL), and aqueous ammonia (14 mL). Next, ethyl orthosilicate (TEOS, 5 mL) was added into the solution under stirring. The mixture was stirred for 1.5 h, and the pH was regulated to 2.0 by adding concentrated hydrochloric acid. Subsequently, a small amount of acetonitrile with 2 g $C_xTA_4H_3[PW_{11}(H_2O)O_{39}]\cdot nH_2O$ was added to the mixture. The mixture was vigorously stirred for 12 h and aged for an additional 24 h at ambient temperature after completion of the addition. After centrifugation, washing, and drying, the precursor of catalyst was obtained. Finally, the precursor was calcinated at 400 °C for 6 h to obtain the catalysts PTA–MCM–41(C_x) (x represents the number of carbon atoms on the alkyl group in template agent, x = 6, 8, 10, 12, 14, 16, and 18).

OTS–PTA–MCM–41(C_x) was synthesized by following procedure. First, 1 g of PTA–MCM–41(C_x) was added to 70 mL of toluene with 15 g OTS. After stirring at ambient temperature for 2 h, the mixture underwent filtration, washing by toluene, and drying, and OTS–PTA–MCM–41(C_x) was successfully synthesized (x represents the number of carbon atoms on the alkyl group in template agent, x = 6, 8, 10, 12, 14, 16, and18).

3.2. Characterization Details

The XRD patterns of catalysts were detected by D/MAX–500X (Rigaku Corporation, Tokyo, Japan) with Cu K_α radiation; the specific parameters were 40 kV and 70 mA. The FT–IR spectra were obtained by Thermo Nicolet 8700 (Thermo Scientific, Waltham, MA, USA) in 400–4000 cm^{-1} region to identify the types of chemical groups in samples. The samples were prepared by the tabbing method. Autosorb–iQ (Quantachrome, Boynton Beach, FL, USA) gas adsorption instrument was used to record the N_2 adsorption–desorption isothermal curves of the samples at 77 K. Before the test, the samples were degassed in a vacuum environment at 373 K for 12 h. The FESEM and TEM images of samples were obtained by HITACHI S–4800 (Hitachi, Tokyo, Japan) field emission scanning electron microscope and JEM–2000EX (JEOL, Tokyo, Japan) Transmission electron microscope. NH_3–TPD was conducted using Micromeritics AutoChem II 2920 (Micromeritics, Norcross, GA, USA) equipment with a thermal conductivity detector (TCD) attached. TG analysis was conducted on a Rubotherm–Dyn THERM thermogravimetric analyzer (TA Instruments, New Castle, DE, USA) under static air atmosphere with a heating rate of 10 °C/min, and the temperature ranged from 100 °C to 800 °C.

3.3. General Catalytic Procedure

3.3.1. Esterification of Free Fatty Acids in the Water

Esterification reaction was carried out with long-chain fatty acids (such as lauric acid, myristic acid, and palmitic acid) and methanol in water. A certain amount of catalyst; 100 mg of lauric acid, myristic acid, and palmitic acid; 5 mL of methanol; and 45 mL of water were added in stainless steel autoclave with Teflon lining at ambient temperature. The mixture was heated to designated temperature under stirring and maintained for a set amount of time. The reaction was quenched by placing the reactor in ice bath. Finally, the mixture was extracted with CH_2Cl_2 (50 mL × 3), and the organic phase was analyzed by gas chromatography (GC).

3.3.2. In Situ Esterification of Fatty Acids in Fermentation Broth

In situ esterification reaction between fatty acids and methanol in fermentation broth was conducted as follows. 45 mL of fermentation broth, 5 mL of methanol, and catalyst were added into stainless steel autoclave with Teflon lining at ambient temperature. The mixture was heated to designated temperature under stirring and maintained for 3 h. The reaction was quenched by placing the reactor in ice bath. Finally, the reaction system was extracted with CH_2Cl_2 (50 mL × 3), and the organic phase was analyzed by GC.

3.4. Cyclic Catalytic Procedure

In a typical cyclic experiment, the used catalyst is obtained by centrifugation and stirred in methanol at ambient temperature for 1 h to regenerate. After that, the catalyst is washed with methanol for several times. Finally, the regenerated catalyst is dried under vacuum at 60 °C for the next reaction.

4. Conclusions

This study designed and synthesized a new type of phosphotungstic acid-functionalized hydrophobic MCM–41 catalyst, OTS–PTA–MCM–41(C_x). The catalyst has a reasonable pore structure, sufficient acidic sites, and can also inhibit the adverse effect of H_2O. The esterification reaction of fatty acids catalyzed by OTS–PTA–MCM–41(C_x) was in accordance with the n–2 rule. The reaction conditions, such as the amount of catalyst, reaction temperature, and time, were also studied in detail to determine the best conditions. The cyclic experiment shows that OTS–PTA–MCM–41(C_{14}) can still maintain more than 97% of the first catalytic performance after five cycles. Finally, the in situ esterification reaction of fermentation broth was catalyzed by mixed OTS–PTA–MCM–41(C_x) catalysts. At optimal reaction conditions, the yields of methyl laurate, methyl myristate, and methyl palmitate reached 91.9%, 89.7%, and 91.2%, which achieved an efficient esterification reaction in the

presence of water solvent. This research is expected to realize the coupling of fermentation and chemical reaction, effective separation of esterified products, and cost reduction. It has reference value for the rational design of hydrophobic solid acid heterogeneous catalyst and green synthesis of biodiesel via esterification reaction in an aqueous and fermentation broth system.

Author Contributions: Conceptualization, methodology, and original draft preparation, D.L. and Q.S.; experiment analysis, D.L. and F.L.; writing—review and editing, D.F. All authors have read and agreed to the published version of the manuscript.

Funding: This research was funded by the National Natural Science Foundation of China (21978311, 21406252) and the Youth Innovation Promotion Association CAS (Y201652).

Data Availability Statement: Data are contained within the article.

Conflicts of Interest: The authors declare no conflicts of interest.

References

1. Rashedi, A.; Khanam, T.; Jonkman, M. On Reduced Consumption of Fossil Fuels in 2020 and Its Consequences in Global Environment and Exergy Demand. *Energies* **2020**, *13*, 6048. [CrossRef]
2. Farghali, M.; Osman, A.I.; Mohamed, I.M.A.; Chen, Z.; Chen, L.; Ihara, I.; Yap, P.S.; Rooney, D.W. Strategies to Save Energy in the Context of the Energy Crisis: A Review. *Environ. Chem. Lett.* **2023**, *21*, 2003–2039. [CrossRef] [PubMed]
3. Debeni Devi, N.; Chaudhuri, A.; Goud, V.V. Algae Biofilm as a Renewable Resource for Production of Biofuel and Value-added Products: A Review. *Sustain. Energy Techn.* **2022**, *53*, 102479. [CrossRef]
4. Mata, T.M.; Martins, A.A.; Caetano, N.S. Microalgae for Biodiesel Production and other Applications: A Review. *Renew. Sust. Energy Rev.* **2010**, *14*, 217–232. [CrossRef]
5. Dey, S.; Reang, N.M.; Das, P.K.; Deb, M. A Comprehensive study on Prospects of Economy, Environment, and Efficiency of Palm Oil Biodiesel as a Renewable Fuel. *J. Clean. Prod.* **2021**, *286*, 124981. [CrossRef]
6. Kang, X.; Guo, X.; You, H. Biodiesel Development in the Global Scene. *Energy Source. Part B* **2014**, *10*, 155–161. [CrossRef]
7. Salaheldeen, M.; Mariod, A.A.; Aroua, M.K.; Rahman, S.M.A.; Soudagar, M.E.M.; Fattah, I.M.R. Current State and Perspectives on Transesterification of Triglycerides for Biodiesel Production. *Catalysts* **2021**, *11*, 1121. [CrossRef]
8. Shaah, M.A.; Hossain, M.S.; Allafi, F.; Ab Kadir, M.O.; Ahmad, M.I. Biodiesel Production from Candlenut Oil using a Non-catalytic Supercritical Methanol Transesterification Process: Optimization, Kinetics, and Thermodynamic Studies. *RSC Adv.* **2022**, *12*, 9845–9861. [CrossRef] [PubMed]
9. Zulqarnain; Yusoff, M.H.M.; Ayoub, M.; Hamza Nazir, M.; Zahid, I.; Ameen, M.; Abbas, W.; Shoparwe, N.F.; Abbas, N. Comprehensive Review on Biodiesel Production from Palm Oil Mill Effluent. *ChemBioEng Rev.* **2021**, *8*, 439–462. [CrossRef]
10. Khalaji, M. Evaluation of Fatty Acid Profiles of Chlorella Vulgaris Microalgae Grown in Dairy Wastewater for Producing Biofuel. *J. Environ. Health Sci.* **2022**, *20*, 691–697. [CrossRef]
11. Zhang, L.; Loh, K.C.; Kuroki, A.; Dai, Y.; Tong, Y.W. Microbial Biodiesel Production from Industrial Organic Wastes by Oleaginous Microorganisms: Current Status and Prospects. *J. Hazard. Mater.* **2021**, *402*, 123543. [CrossRef]
12. Chaowamalee, S.; Yan, N.; Ngamcharussrivichai, C. Propylsulfonic Acid-Functionalized Mesostructured Natural Rubber/Silica Nanocomposites as Promising Hydrophobic Solid Catalysts for Alkyl Levulinate Synthesis. *Nanomaterials* **2022**, *12*, 604. [CrossRef]
13. Lee, A.F.; Wilson, K. Recent Developments in Heterogeneous Catalysis for the Sustainable Production of Biodiesel. *Catal. Today* **2015**, *242*, 3–18. [CrossRef]
14. Zheng, Y.; Zheng, Y.; Yang, S.; Guo, Z.; Zhang, T.; Song, H.; Shao, Q. Esterification Synthesis of Ethyl Oleate Catalyzed by Brønsted acid–surfactant-combined Ionic Liquid. *Green Chem. Lett. Rev.* **2017**, *10*, 202–209. [CrossRef]
15. Björk, E.M.; Militello, M.P.; Tamborini, L.H.; Coneo Rodriguez, R.; Planes, G.A.; Acevedo, D.F.; Moreno, M.S.; Odén, M.; Barbero, C.A. Mesoporous Silica and Carbon Based Catalysts for Esterification and Biodiesel Fabrication—The Effect of Matrix Surface Composition and Porosity. *Appl. Catal. A-Gen.* **2017**, *533*, 49–58. [CrossRef]
16. Shi, S.; Valle-Rodriguez, J.O.; Khoomrung, S.; Siewers, V.; Nielsen, J. Functional Expression and Characterization of Five Wax Ester Synthases in Saccharomyces Cerevisiae and Their Utility for Biodiesel Production. *Biotechnol. Biofuels* **2012**, *5*, 7. [CrossRef] [PubMed]
17. Gao, Q.; Yang, J.L.; Zhao, X.R.; Liu, S.C.; Liu, Z.J.; Wei, L.J.; Hua, Q. Yarrowia Lipolytica as a Metabolic Engineering Platform for the Production of Very-Long-Chain Wax Esters. *J. Agric. Food Chem.* **2020**, *68*, 10730–10740. [CrossRef] [PubMed]
18. Liu, H.; Yu, C.; Feng, D.; Cheng, T.; Meng, X.; Liu, W.; Zou, H.; Xian, M. Production of Extracellular Fatty Acid using Engineered Escherichia coli. *Microb. Cell Fact.* **2012**, *11*, 41. [CrossRef] [PubMed]

19. Gaide, I.; Makareviciene, V.; Sendzikiene, E.; Kazancev, K. Natural Rocks–Heterogeneous Catalysts for Oil Transesterification in Biodiesel Synthesis. *Catalysts* **2021**, *11*, 384. [CrossRef]
20. Hsiao, M.; Kuo, J.; Hsieh, S.; Hsieh, P.; Hou, S. Optimized Conversion of Waste Cooking oil to Biodiesel Using Modified Calcium Oxide as Catalyst via a Microwave Heating System. *Fuel* **2020**, *266*, 117114. [CrossRef]
21. Hassan, S.Z.; Vinjamur, M. Concentration-independent Rate Constant for Biodiesel Synthesis from Homogeneous-catalytic Esterification of Free Fatty Acid. *Chem. Eng. Sci.* **2014**, *107*, 290–301. [CrossRef]
22. Li, M.; Lu, P.; Ye, C.; Chen, J.; Qiu, T. Amphiphilic Heteropolyacid-based Sulfonic Acid-functionalised Ionic Liquids as Efficient Catalysts for Biodiesel Production. *Fuel* **2023**, *354*, 129269. [CrossRef]
23. Zhang, Q.; Luo, Q.; Wu, Y.; Yu, R.; Cheng, J.; Zhang, Y. Construction of a Keggin Heteropolyacid/Ni-MOF Catalyst for Esterification of Fatty Acids. *RSC Adv.* **2021**, *11*, 33416–33424. [CrossRef] [PubMed]
24. Guo, L.; Xie, W.; Gao, C. Heterogeneous $H_6PV_3MoW_8O_{40}$/AC-Ag Catalyst for Biodiesel Production: Preparation, Characterization and Catalytic Performance. *Fuel* **2022**, *316*, 123352. [CrossRef]
25. Leng, Y.; Wang, J.; Zhu, D.; Wu, Y.; Zhao, P. Sulfonated Organic Heteropolyacid Salts: Recyclable Green Solid Catalysts for Esterifications. *J. Mol. Catal. A-Chem.* **2009**, *313*, 1–6. [CrossRef]
26. Mohan, V.; Pramod, C.V.; Suresh, M.; Prasad Reddy, K.H.; Raju, B.D.; Rama Rao, K.S. Advantage of Ni/SBA-15 Catalyst over Ni/MgO Catalyst in terms of Catalyst Stability due to Release of Water during Nitrobenzene Hydrogenation to Aniline. *Catal. Commun.* **2012**, *18*, 89–92. [CrossRef]
27. Ruan, S.; Chen, S.; Lu, J.; Zeng, Q.; Liu, Y.; Yan, D. Waterproof Geopolymer Composites Modified by Hydrophobic Particles and Polydimethylsiloxane. *Compos. Part B-Eng.* **2022**, *237*, 109865. [CrossRef]
28. Li, B.; Ma, W.; Liu, J.; Zuo, S.; Li, X. Preparation of MCM-41 Incorporated with Lacunary Keggin Polyoxometalate and its Catalytic Performance in Esterification. *J. Colloid Interf. Sci.* **2011**, *362*, 42–49. [CrossRef] [PubMed]
29. Brasil, H.; Carvalho, A.L.G.d.; Costa, F.F.; Nascimento, L.A.S.d.; Mhadmhan, S.; Pineda, A.; Luque, R.; Valença, G.P. Preparation of Novel Mesoporous Ca/P MCM-41-based Materials for Mechanochemical Diphenyl Sulfide Oxidation. *Micropor. Mesopor. Mat.* **2020**, *297*, 110017. [CrossRef]
30. Alshorifi, F.T.; Tobbala, D.E.; El-Bahy, S.M.; Nassan, M.A.; Salama, R.S. The Role of Phosphotungstic Acid in Enhancing the Catalytic Performance of UiO-66 (Zr) and its Applications as an Efficient Solid Acid Catalyst for Coumarins and Dihydropyrimidinones Synthesis. *Catal. Commun.* **2022**, *169*, 106479. [CrossRef]
31. Zhu, W. Phosphotungstic Acid Passivated Enhanced Photocatalytic Performance of ZnS Nanoparticles under Solar Light. *Solid State Sci.* **2021**, *118*, 106406. [CrossRef]
32. Karthikeyan, G.; Pandurangan, A. Heteropolyacid ($H_3PW_{12}O_{40}$) Supported MCM-41: An Efficient Solid Acid Catalyst for the Green Synthesis of Xanthenedione Derivatives. *J. Mol. Catal. A-Chem.* **2009**, *311*, 36–45. [CrossRef]
33. Andas, J.; Ekhbal, S.H.; Ali, T.H. MCM-41 Modified Heterogeneous Catalysts from Rice Husk for Selective Oxidation of Styrene into Benzaldehyde. *Environ. Technol. Inno.* **2021**, *21*, 101308. [CrossRef]
34. Wang, R.; Wan, J.; Li, Y.; Sun, H. An Improvement of MCM-41 Supported Phosphoric Acid Catalyst for Alkylation Desulfurization of Fluid Catalytic Cracking Gasoline. *Fuel* **2015**, *143*, 504–511. [CrossRef]
35. Ma, T.; Yun, Z.; Xu, W.; Chen, L.; Li, L.; Ding, J.; Shao, R. Pd-$H_3PW_{12}O_{40}$/Zr-MCM-41: An Efficient Catalyst for the Sustainable Dehydration of Glycerol to Acrolein. *Chem. Eng. J.* **2016**, *294*, 343–352. [CrossRef]
36. Yu, Y.; Sun, D.; Wang, S.; Xiao, M.; Sun, L.; Meng, Y. Heteropolyacid Salt Catalysts for Methanol Conversion to Hydrocarbons and Dimethyl Ether: Effect of Reaction Temperature. *Catalysts* **2019**, *9*, 320. [CrossRef]
37. Zapata, P.A.; Faria, J.; Ruiz, M.P.; Jentoft, R.E.; Resasco, D.E. Hydrophobic Zeolites for Biofuel Upgrading Reactions at the Liquid-liquid Interface in Water/oil Emulsions. *J. Am. Chem. Soc.* **2012**, *134*, 8570–8578. [CrossRef] [PubMed]
38. Singh, R.; Dutta, P.K. Use of Surface-modified Zeolite Y for Extraction of Metal Ions from Aqueous to Organic Phase. *Micropor. Mesopor. Mat.* **1999**, *32*, 29–35. [CrossRef]
39. Adam, F.; Sek, K.L. Heterogenization of Indium for the Friedel-Craft Benzoylation of Toluene. *Chinese J. Catal.* **2012**, *33*, 1802–1808. [CrossRef]
40. Lin, Y.; Cheng, T.; Lin, W.; Lo, H.; Lo, K.; Chen, C.; Lin, K. Molecular Sieve Material from Liquid–crystal-display Waste Glass and Silicon Carbide Sludge via Hydrothermal Process with Alkali Fusion Pretreatment. *J. Mater. Cycles Waste* **2021**, *23*, 1081–1089. [CrossRef]
41. Bharathi, M.; Mathivathani, S.; Indira, S.; Vinoth, G.; Christopher Leslee, D.B.; Shanmuga Bharathi, K. Anchoring of a Nickel Schiff Base Complex with Mixed Ligands on MCM-41 as a Heterogeneous Catalyst for the Synthesis of Quinoxaline Derivatives by Various Energies. *Polyhedron* **2023**, *229*, 116188. [CrossRef]
42. Kukovecz, Á.; Balogi, Z.; Kónya, Z.; Toba, M.; Lentz, P.; Niwa, S.I.; Mizukami, F.; Molnar, A.; Nagy, J.B.; Kiricsi, I. Synthesis, Characterisation and Catalytic Applications of Sol-gel Derived Silica-phosphotungstic Acid Composites. *Appl. Catal. A-Gen.* **2002**, *228*, 83–94. [CrossRef]
43. Meng, F.; Zhang, Y.; Li, J.; Fu, W.; Zhang, J. Preparation of a Liquefied Banana Pseudo-stem Based PVAc-nanosilica Hybrid Membrane and its Modification by Octadecyltrichlorosilane. *RSC Adv.* **2016**, *6*, 94170–94176.
44. Senoymak Tarakcı, M.I.; Ilgen, O. Esterification of Oleic Acid with Methanol Using $Zr(SO_4)_2$ as a Heterogeneous Catalyst. *Chem. Eng. Technol.* **2018**, *41*, 845–852. [CrossRef]

45. Patel, A.; Singh, S. Undecatungstophosphate Anchored to MCM-41: An Ecofriendly and Efficient Bifunctional Solid Catalyst for Non-solvent Liquid-phase Oxidation as well as Esterification of Benzyl alcohol. *Micropor. Mesopor. Mat.* **2014**, *195*, 240–249. [CrossRef]
46. Szegedi, Á.; Popova, M. Toluene Hydrogenation over Nickel-containing MCM-41 and Ti-MCM-41 Materials. *J. Porous Mat.* **2009**, *17*, 663–668. [CrossRef]